In-time implicit–explicit algorithm for nonlinear finite element analysis

J.L. Curiel Sosa*, E. de Souza Neto, D.R.J. Owen

Civil and Computational Engineering Centre, University of Wales–Swansea, Singleton Park, Swansea SA2 8PP, UK

Abstract

A scheme to solve finite element problems with certain nonlinearities has been developed. It consists of a combination of the two general strategies – explicit and implicit – in such a manner that when the implicit process starts to diverge, the explicit one is activated and executed until proper convergence is reached. Partitioning of the mesh into parts or groups of nodes for separate implicit or explicit treatment of solution is not considered in this work. The formulation is presented initially and its implementation is validated by the analysis of a key numerical example.

Keywords: Explicit; Implicit; Nonlinear; Large deformations; Contact; Buckling

1. Introduction

Some problems in finite element analysis may not be solved readily by implicit methods, such as a sharp pointed edge contacting a concave surface, and for such cases direct integration of the momentum equations (explicit) offers an alternative scheme of solution. In this paper, the idea of executing an implicit method until divergence arises and at that point continuing to solve with an explicit method is highlighted. Processing flow is returned to the implicit scheme (IMP) when the divergency condition has passed.

The aim of this article is to illustrate the implicit/explicit (IMP/EXP) algorithm without considering contact problems at this time. A connection between the Newton–Raphson method (NRM) (implicit) and the central difference method (CDM) (explicit) has been elected. A description of the implicit and explicit schemes, their coded form, and their connection is presented. Finally, a numerical geometrically nonlinear example of arch buckling is presented.

2. Implicit formulation

A solution of the weak form of the momentum equations by the NRM is used. The implicit algorithm includes large deformations and is based upon a pseudo-time discretization [1] considering the transition of deformation between two time points. Thus, if a time increment $[t_n, t_{n+1}]$ and set of internal variables $\boldsymbol{\alpha}_n$ at t_n are given, then the deformation gradient $\mathbf{F}_{n+1}$ (at the end of interval $[t_n, t_{n+1}]$) determines stresses $\boldsymbol{\sigma}(t_{n+1})$ and internal variables only through the integration algorithm $\boldsymbol{\sigma}_{\mathrm{n+1}} = \hat{\boldsymbol{\sigma}}(\boldsymbol{\alpha}_{\mathrm{n}}, \mathrm{F}_{\mathrm{n+1}})$:

$$\boldsymbol{R}(\boldsymbol{u}_{n+1}) = \mathbf{f}^{int}(\boldsymbol{u}_{n+1}) - \mathbf{f}^{ext}_{n+1} = 0 \tag{1}$$

$$\mathbf{f}^{int}(\boldsymbol{u}_{n+1}) = \bigwedge_{e=1}^{nelem} \left\{ \int_{\varphi_{n+1}(\Omega^{(e)})} \mathbf{B}^T \boldsymbol{\sigma}(\boldsymbol{\alpha}_n, \mathbf{F}(\boldsymbol{u}_{n+1}))\mathrm{d}v \right\} \tag{2}$$

$$\mathbf{f}^{ext}_{n+1} = \bigwedge_{e=1}^{nelem} \left\{ \int_{\varphi_{n+1}(\Omega^{(e)})} \mathbf{N}^T \boldsymbol{b}_{n+1} dv + \int_{\partial\varphi_{n+1}(\Omega^{(e)})} \mathbf{N}^T \boldsymbol{q}_{n+1} \mathrm{d}s \right\} \tag{3}$$

where φ_{n+1} $(\Omega^{(e)})$ is the current deformed domain. For details of linearization of Eq. (1) to obtain Eq. (4), see de Souza et al. [2]. A generic iteration of the NRM to solve the standard linear system involves the following computations:

$$\mathbf{K}_T \delta \boldsymbol{u}^{(k)} = -\boldsymbol{R}^{(k-1)} \tag{4}$$

where $\mathbf{K}_T$ is obtained through $\mathbf{G}$ (discrete (full) spatial gradient operator) [2] and is of the form

* Corresponding author. Tel.: +44 7816 331479; E-mail: 205728@swansea.ac.uk

Computational Fluid and Solid Mechanics 2005
K.J. Bathe (Editor)

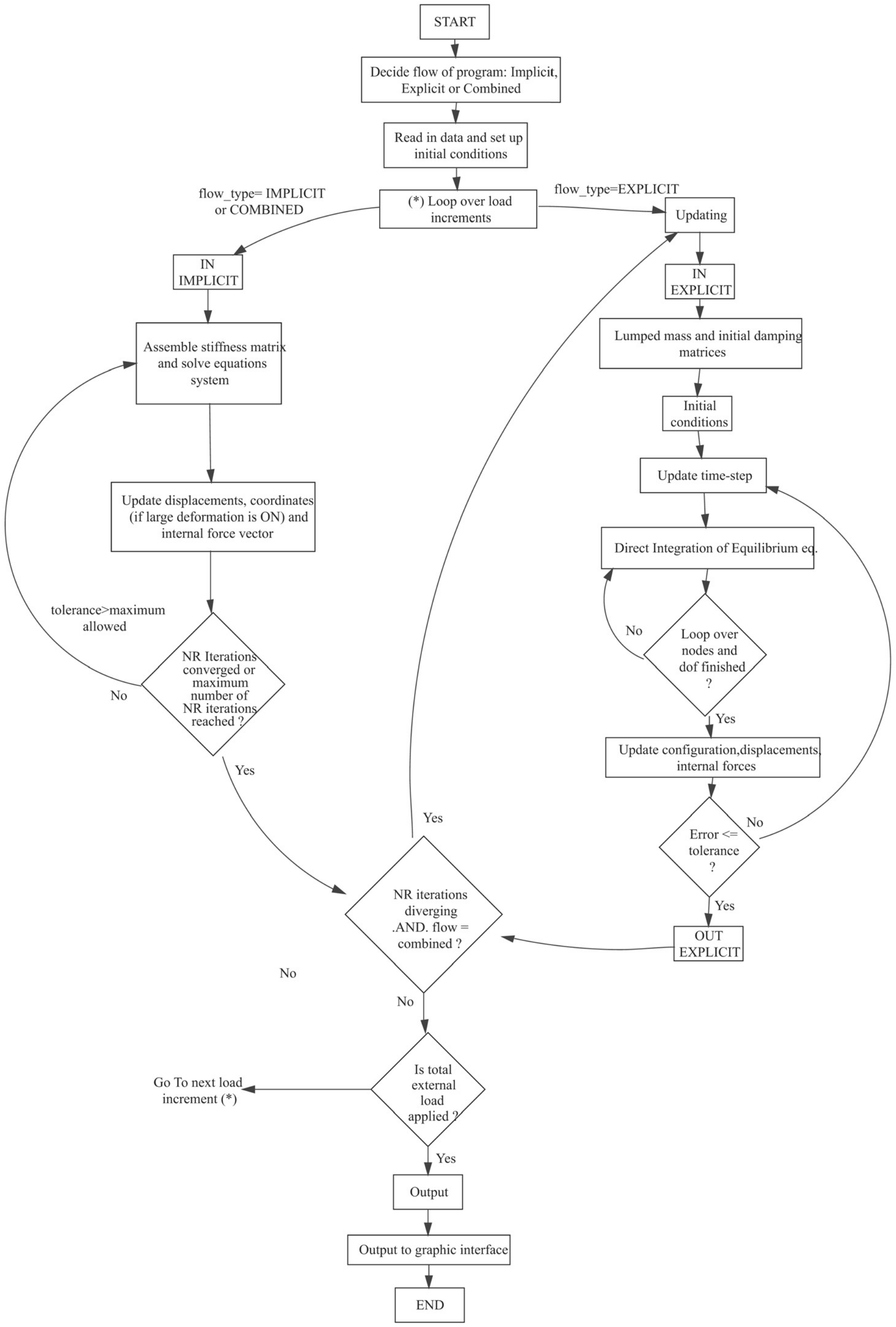

Fig. 1. Combined implicit/explicit algorithm.

$$\mathbf{K}_T = \bigwedge_{\mathrm{e}=1}^{\mathrm{nelem}} \left\{ \int_{\varphi_{n+1}(\Omega^{(e)})} \mathbf{G}^T \mathbf{a} \mathbf{G} \mathrm{d}v \right\} \tag{5}$$

The fourth-order tensor **a** is the consistent spatial tangent modulus and, in cartesian components, is defined by Eq. (6) at the end of iteration:

$$a_{ijkl} = \frac{1}{J} \frac{\partial \tau_{ij}}{\partial F_{km}} F_{lm} - \sigma_{il} \delta_{jk} \tag{6}$$

The computation of the consistent spatial tangent moduli is given by

$$\hat{a}_{ijkl} = \frac{1}{J} \frac{\partial \hat{\tau}_{ij}}{\partial F_{km}} F_{lm} - \sigma_{il} \delta_{jk} \tag{7}$$

Assembling of the element stiffness matrices:

$$\mathbf{k}_T^{(e)} = \sum_{i=1}^{n_{gaus}} \omega_i j_i \mathbf{G}_i^T \hat{\mathbf{a}}_i \mathbf{G}_i \tag{8}$$

Solving the linearized equilibrium Eq. (4):

$$\boldsymbol{u}_{n+1}^{(k)} = \boldsymbol{u}_{n+1}^{(k-1)} + \delta \boldsymbol{u}^{(k)} \tag{9}$$

$$\boldsymbol{\varepsilon}_{n+1}^{(k)} = \mathbf{B} \boldsymbol{u}_{n+1}^{(k)} \tag{10}$$

Updating the deformation gradient:

$$\mathbf{F}_{n+1}^{(k)} = (\mathbf{I} - \nabla_x \boldsymbol{u}_{\mathbf{n+1}}^{(\mathbf{k})})^{-\mathbf{1}} \tag{11}$$

Use of the constitutive integration algorithm to update the stress and other state variables:

$$\boldsymbol{\sigma}_{n+1}^{(k)} = \hat{\boldsymbol{\sigma}}(\boldsymbol{\alpha}_n, \mathbf{F}_{n+1}^{(k)}) \tag{12}$$

$$\boldsymbol{\alpha}_{n+1}^{(k)} = \hat{\boldsymbol{\alpha}}(\boldsymbol{\alpha}_n, \mathbf{F}_{n+1}^{(k)}) \tag{13}$$

Internal forces for each element:

$$\boldsymbol{f}_{(e)}^{int} = \sum_{j=1}^{n_{gaus}} \xi_j J_j B_j^T \boldsymbol{\sigma}_{n+1,j}^{(k)} \tag{14}$$

Gathering of element internal forces vector and updating the residual. If iterations diverge, then go to the EXP scheme (see Fig. 1) or else check the stop criterium

$$\frac{\|\boldsymbol{f}^{ext} - \boldsymbol{f}^{int}\|}{\|\boldsymbol{f}^{ext}\|} \le \epsilon$$

Then the solution for the current external load is reached and values for this load are taken from the last iteration $(\bullet)_{n+1} = (\bullet)_{n+1}^{(k)}$

3. Explicit formulation

The EXP sub-algorithm is activated in case of divergency of IMP. Once the solution is reached, flow is returned back to IMP execution if the external load has not been totally applied (Fig. 1).

The central differences method (CDM) consists of integrating directly the spatially discretized dynamic equilibrium equation at time t^n:

$$\mathbf{M}\ddot{\mathbf{u}}(t_n) + \mathbf{C}\dot{\mathbf{u}}(t_n) + \mathbf{f}^{int}(\mathbf{u}_n) = \mathbf{f}^{ext} \tag{15}$$

$$\dot{\mathbf{u}}(t_{n-1/2}) = \frac{\mathbf{u}(t_n) - \mathbf{u}(t_{n-1})}{\Delta t_n} \tag{16}$$

$$\dot{u}_{i,n+1/2} = \left[\frac{M_{ii}}{\Delta t_n} + \frac{C_{ii}}{2}\right]^{-1} \cdot \left[\left[\frac{M_{ii}}{\Delta t_n} - \frac{C_{ii}}{2}\right] \dot{u}_{i,n-1/2} + f_i^{ext} - f_i^{int}(u_n)\right] \tag{17}$$

$$\mathbf{u}(t_{n+1}) = \mathbf{u}(t_n) + \dot{\mathbf{u}}_{n+1/2} \Delta t_{n+1} \tag{18}$$

A lumped mass matrix is elected such that

$$\mathbf{M} = \bigwedge_{e=1}^{nelem} \int_{\Omega_{(e)}} \rho_0 \mathbf{N}_{(e)}^T \mathbf{N}_{(e)} d\omega \tag{19}$$

The damping matrix is chosen to be mass-proportional as

$$\mathbf{C} = \alpha \mathbf{M} \tag{20}$$

The time step is elected as

$$\Delta t(t_{n+1}) \le \Delta t_c(t_{n+1}) = \frac{2}{max_i\{\omega_i(t_n)\}} \tag{21}$$

where the natural frequencies are determined from the homogeneous problem [3]. Its analytical solution is in the form $u(t) = \tilde{u} e^{-j\omega t}$ ($\mathrm{j} = \sqrt{-1}$). Substituting in Eq. (22), an eigenvalue problem is obtained:

$$\mathbf{M}\ddot{\mathbf{u}} + \mathbf{K}\mathbf{u} = 0 \tag{22}$$

Introducing the analytical solution form leads to

$$\left|-\omega^2 \mathbf{M} + \mathbf{K}\right| = 0 \tag{23}$$

An approximation of the stiffness is taken as

$$K_{ii}(t_n) \simeq \frac{f_i^{int}(u_n) - f_i^{int}(u_{n-1})}{\dot{u}_i^{n-1/2} \Delta t_n} \tag{24}$$

and of the frequencies as

$$\omega_i(t_n) = \sqrt{\frac{K_{ii}(t_n)}{M_{ii}}} \tag{25}$$

4. Transition implicit/explicit

The last converged iteration at IMP (displacement $\tilde{\mathbf{u}}$) is transferred to EXP as initial conditions. Thus, the final internal forces and displacements, from IMP, are

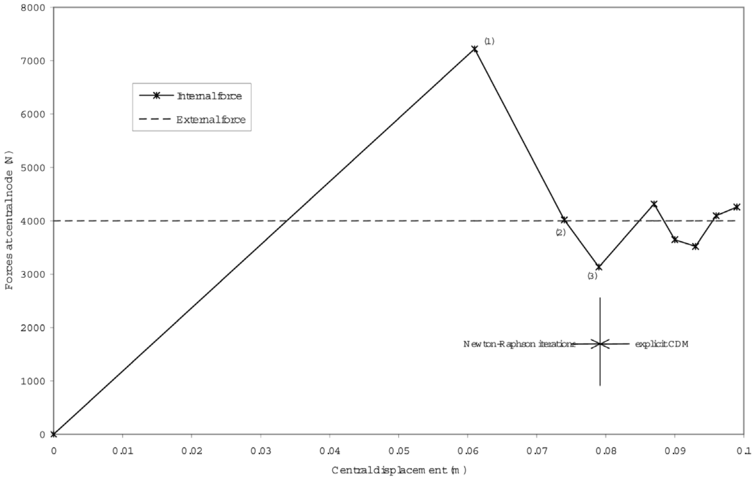

Fig. 2. Vertical nodal forces versus displacement in absolute value at the top central node.

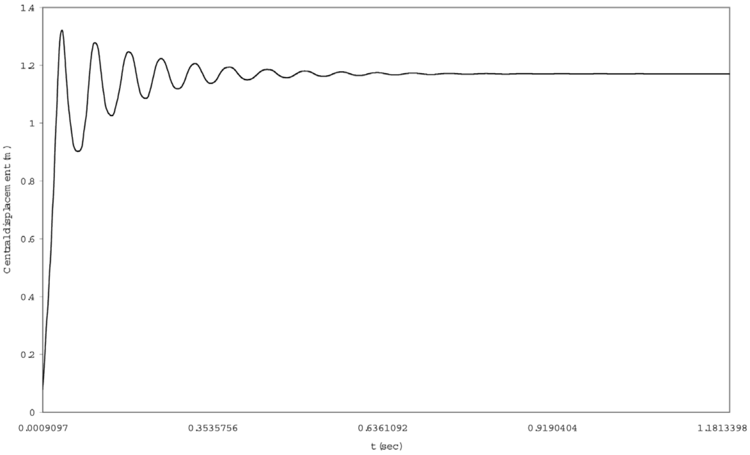

Fig. 3. Absolute value of deflection at the central node. Plot starts when EXP is initiated after three IMP iterations (see Fig. 2).

used to determine initial accelerations and velocities for EXP:

$$\begin{array}{ccc} \mathbf{f}^{int}(\tilde{\mathbf{u}}) & \rightarrow & \mathbf{f}^{int}(0) \\ \tilde{\mathbf{u}} & \rightarrow & \mathbf{u}(0) \end{array}$$

The initial velocities for EXP are approximated as follows:

$$\begin{aligned} \ddot{u}_i(0) &= \frac{f_i^{ext} - f_i^{int}(0)}{M_{ii}} \\ \dot{u}_i(0) &= \ddot{u}_i(0)\Delta t(0) + \dot{u}_i^- \\ \dot{u}_i^-(0) &= 0.0 \end{aligned} \qquad (0)$$

where $\Delta t(0)$ is the initial time step. After the first iteration, an adaptive step in time is carried out. A flowchart of the IMP/EXP algorithm is represented in Fig. 1.

5. Numerical example

The buckling of an aluminium alloy (Young modulus $E = 6.895 \times 10^4$ MPa, poisson ratio $\nu = 0.34$, and density $\rho = 2700\,\mathrm{kg/m^3}$) arch is presented. An external point load (up to a magnitude 4000 N that causes the snap-through of the arch) is applied in the center of the arch. Other geometric values are cross-sectional area $A = 25\,806 \times 10^{-4}\,\mathrm{m^2}$, inertia moment $I = 5.54 \times 10^{-7}\,\mathrm{m^4}$, thickness $t = 0.0508$ m, arch radius $R = 5.08$ m, and arch angle 60°. Calhoun and DaDeppo [4] simulated its pre-buckling behavior and a further

Fig. 4. Vertical displacement at the midpoint ($|\mathbf{f}^{int}_{central\,node,y}| = 4000\,\mathrm{N}$).

development was performed by Pi and Trahair [5], carrying out simulations after the buckling point. The NRM started to diverge at a deflection $|\delta_{crit}| = 0.076\,\mathrm{m}$ (which corresponds to an internal nodal force at vertical direction $|\mathbf{f}^{int}_{central\,node,y}| = 2781.917\,\mathrm{N}$, and, hence, EXP is initialized (with the last converged solution of NRM indicated in Fig. 2 at point 3). The final deformation may be observed in Fig. 3. Convergency to solution $|\delta_{sol}| = 1.17\,\mathrm{m}$ (absolute value of deflection at the central node) is reached (see Fig. 4).

6. Concluding remarks

An algorithm that considers the combination in time of the two general strategies of solution (implicit and explicit) has been presented, in particular for the analysis of large deformations where geometrically nonlinear buckling results in divergency of the NRM. Practical application of this algorithm might also include the solution of contact problems in which sharp pointed edges and curved concave surfaces are involved.

References

[1] Simo JC, Hughes TJR. Computational Inelasticity, 2nd edn. New York: Springer, 1998.
[2] De Souza E, Peric D, Owen DRJ. Computational plasticity.
[3] Zienkiewicz OC, Taylor RL. The Finite Element Method, Vol. 1. Oxford, UK, Woburn, MA: Butterworth-Heinemann, 2000.
[4] Calhoun PR, DaDeppo DA. Nonlinear finite element analysis of clamped arches. J Struct Engng ASCE 1983;109:599–612.
[5] Pin Y-L, Trahair NS. Nonlinear buckling and postbuckling of elastic arches. Engng Struct 1998;20:571–579.